Rotational band built on the $\frac{1}{2}[660](i_{13/2})$ configuration in ^{179}Au

L. T. Song, X. H. Zhou, Y. H. Zhang, Y. X. Guo, X. G. Lei, and Z. Y. Sun
Institute of Modern Physics, Chinese Academy of Science, Lanzhou 730000, People's Republic of China

M. Oshima, T. Toh, A. Osa, M. Koizumi, J. Katakura, Y. Hatsukawa, and M. Matsuda
Japan Atomic Energy Research Institute, Tokai, Ibaraki 319-1195, Japan

M. Sugawara
Chiba Institute of Technology, Narashino, Chiba 275-0023, Japan
(Received 18 November 2003; published 12 March 2004)

High-spin states in ^{179}Au have been studied experimentally using the ^{149}Sm(^{35}Cl,5n) fusion-evaporation reaction at beam energies of 164−180 MeV. A rotational band built on the $\frac{1}{2}[660](i_{13/2})$ Nilsson orbital has been established for ^{179}Au. Properties of the $\frac{1}{2}[660](i_{13/2})$ bands in the odd-A Au nuclei are discussed with an emphasis on the evolution of bandhead energy and deformation while changing neutron number.

DOI: 10.1103/PhysRevC.69.037302 PACS number(s): 27.70.+q, 21.10.Re, 23.20.Lv

Neutron-deficient nuclei near the $Z=82$ shell closure are well known to exhibit coexistence between an oblate or nearly spherical shape and a prolate shape [1–4]. Gold nuclei with $Z=79$ have provided rich information on the shape coexistence and shape transition along the yrast line. For the heavier odd-A Au nuclei with $A>187$, the low-energy level structure shows typical character of single-particle excitations, and rotational bands of collectivity are observed experimentally with increasing excitation energies or angular momenta [5–9]. It is found experimentally that prolate shapes are lower in energy for lighter isotopes. The level structures in ^{181,183,185,187}Au consist mainly of prolate rotational bands, and the intruder $\frac{1}{2}[541](h_{9/2})$ and $\frac{1}{2}[660](i_{13/2})$ bands are most strongly populated [4,10–12]. Recently, excited states in the proton-unbound ^{173,175,177}Au nuclei were identified [11]. While the yrast lines of ^{175}Au and ^{177}Au undergo a shape transition from oblate or spherical to prolate at low spin and are dominated at high spin by a prolate band built upon the intruder $\frac{1}{2}[660](i_{13/2})$ proton orbital, no sign of collectivity was observed in ^{173}Au isotope [11]. The purpose of the present work is to search for the decoupled bands based on the $\frac{1}{2}[541](h_{9/2})$ and $\frac{1}{2}[660](i_{13/2})$ intruder orbitals in ^{179}Au, and thus complete the evolution of bandhead energies and deformations of these intruder bands while changing neutron number in odd-A Au isotopes. Prior to this work, little information on the excited levels and band structure in ^{179}Au was available. The ground state of ^{179}Au was assumed to be the $5/2^-$ member of the intruder $\frac{1}{2}[541](h_{9/2})$ band [11]. In ^{183}Tl α-decay studies, two low-energy levels were suggested for ^{179}Au [13–15]. The present work confirms earlier unpublished indications of an $i_{13/2}$ band in ^{179}Au [11].

The excited states in ^{179}Au were populated via the ^{149}Sm(^{35}Cl,5n)^{179}Au reaction. The ^{35}Cl beam was provided by the tandem accelerator at the Japan Atomic Energy Research Institute (JAERI). The target is an isotopically enriched ^{149}Sm metallic foil of 1.5 mg/cm^2 thickness with a 5.0 mg/cm^2 Pb backing. A γ-ray detector array, comprising 13 HPGe's with BGO anti-Compton shields and three LOAX detectors being sensitive to low-energy γ rays, was used. To obtain DCO ratios, the detectors were divided into three groups of which the angle positions (and detector number at that angle) were 90° (2), ±72° (6), ±35° (8) with respect to the beam axis. The detectors were calibrated with ^{60}Co, ^{133}Ba, and ^{152}Eu standard sources; typical energy resolution was about 2.0−2.7 keV at full width at half maximum for the 1332.5-keV line. In order to identify the in-beam γ rays belonging to ^{179}Au and to determine the optimum beam energy to produce ^{179}Au, first, we measured the relative γ-ray yields at the beam energies of 164 and 178 MeV. Then, the beam energy of 180 MeV, at which the yield of ^{179}Au was expected to be a maximum, was chosen to populate the high-spin states in ^{179}Au. γ-γ-t and X-γ-t coincidence measurements were performed at beam energy of 180 MeV. A total of about 250×10^6 coincidence events were accumulated. After accurate gain matching, these coincidence events were sorted into a symmetric matrix and a DCO matrix for off-line analysis.

The measured relative γ-ray yields at different beam energies, combined with Au K x-ray coincident information and

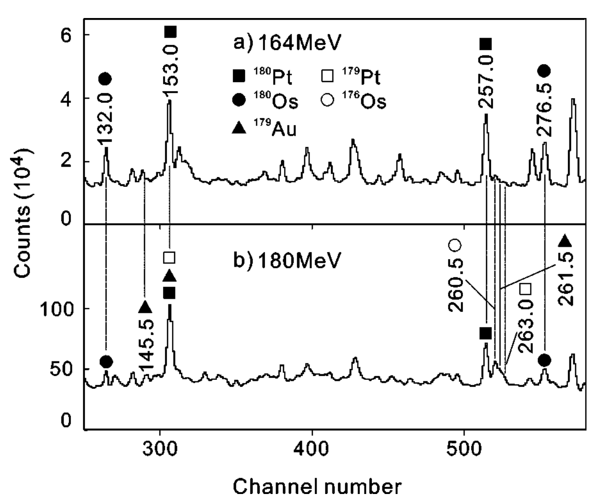

FIG. 1. Total projection spectra at beam energies of 164 MeV and 180 MeV.

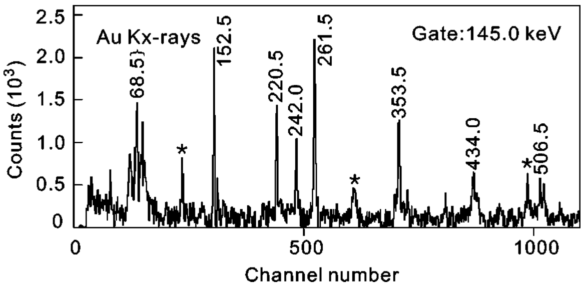

FIG. 2. *γ-ray* coincidence spectrum obtained by gating on the 145.0-keV transition. The asterisks (*) indicate contaminations.

the existing knowledge of band properties in neighboring odd-Z nuclei, helped us assign the γ-ray cascade to ^{179}Au. Because of severe competition from fission and many competing evaporation channels open in the present reaction, the γ-ray spectra in this experiment were very complex. We therefore used coincidence mode in the excitation function measurements. The partial total projection spectra measured at beam energies of 164 and 180 MeV are displayed in Fig. 1. As shown in Fig. 1, the relative yields of known γ rays from ^{180}Pt and ^{180}Os, produced in the $^{149}\mathrm{Sm}(^{35}\mathrm{Cl},1p3n)^{180}\mathrm{Pt}$ and $^{149}\mathrm{Sm}(^{35}\mathrm{Cl},3p1n)^{180}\mathrm{Os}$ reactions, respectively, decrease apparently at the higher beam energy, while those from the $^{149}\mathrm{Sm}(^{35}\mathrm{Cl},1p4n)^{179}\mathrm{Pt}$ and $^{149}\mathrm{Sm}(^{35}\mathrm{Cl},\alpha 1p3n)^{176}\mathrm{Os}$ reaction channels are much enhanced with increasing beam energy. The relative yields of the 145.0- and 261.5-keV γ rays have a similar pattern with beam energy as the γ rays from ^{179}Pt and ^{176}Os nuclei, indicating that the 145.0- and 261.5-keV γ rays should originate from a reaction channel evaporating five particles. A γ-ray spectrum gated on the 145.0-keV transition is displayed in Fig. 2, in which all γ rays are in coincidence with the Au K x rays and the 145.0-, 152.5-, 220.5- (or 242.0-), 261.5-, 353.5-, 434.0-, and 506.5-keV transitions are in coincidence with one another. Therefore, the γ rays shown in Fig. 2 are assigned to ^{179}Au. The level scheme of ^{179}Au, including eight γ rays, is proposed and shown in Fig. 3. The placement of transitions and levels is determined from the γ-ray coincidence relationships. The ordering of transitions in the band is determined according to the γ-ray relative intensities. The relative transition intensities were extracted from gated spectra. Figure 4 compares partial level schemes of ^{177,179,181,183,185}Au, strongly suggesting that the band of ^{179}Au fits well into the systematics of the $\frac{1}{2}[660](i_{13/2})$ intruder bands observed in the heavier odd-A Au isotopes. Based on the similarities as shown in Fig. 4, spins and parities are proposed tentatively to

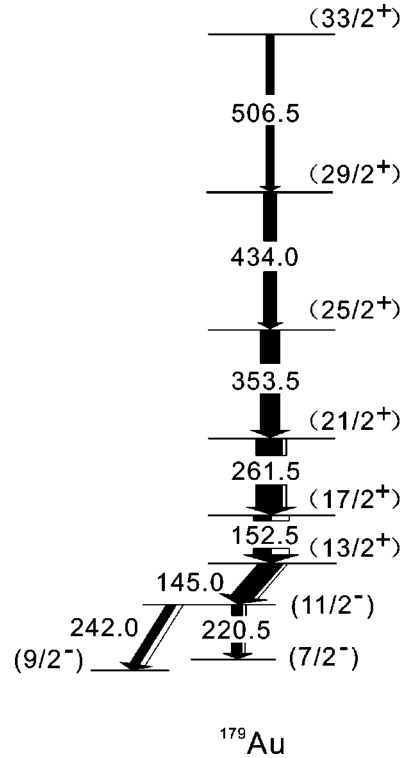

FIG. 3. Level scheme for ^{179}Au.

the levels in ^{179}Au. The transition intensities below the $13/2^+$ level are apparently smaller than those above the $13/2^+$ level, indicating that there are other unobserved branches to depopulate the $13/2^+$ level. Due to the poor statistics and bad layout of the detectors with only two detectors positioned at 90° with respect to the beam direction, we could not extract reliable DCO ratios from coincidence data for the transitions assigned to ^{179}Au. However, the transition multipolarities, as suggested from Fig. 4, are consistent with the results deduced from the intensity balances. The intensities of the 152.5- and 261.5-keV transitions should be same in the spectrum gated on the 353.5-keV γ ray. Assuming an $E2$ character for the 261.5-keV transition, we obtain a total internal conversion coefficient of 0.9 for the 152.5-keV transition, whose theoretical values are 0.14, 0.99, and 2.24 for $E1$, $E2$, and $M1$ multipolarities, respectively. Therefore, we assign a likely $E2$ character to the 152.5-keV transition. The estimated total conversion coefficient favors the 145.0-keV transition to be an $E1$ character.

In the heavier odd-A Au nuclei, the $h_{9/2}$, $f_{7/2}$, and $i_{13/2}$ bands have been commonly observed, among which the $i_{13/2}$

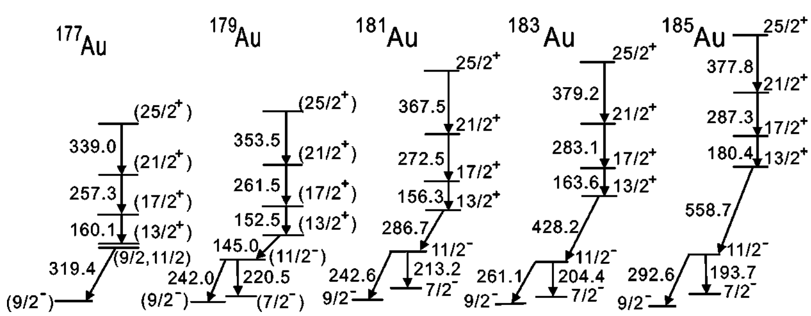

FIG. 4. Partial level schemes of ^{177}Au, ^{179}Au, ^{181}Au, ^{183}Au, and ^{185}Au.

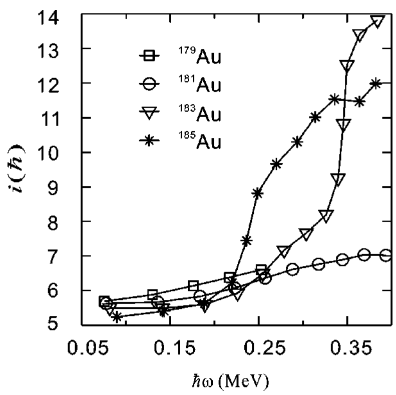

FIG. 5. Extracted alignment for the $\pi i_{13/2}$ rotational bands in ^{179}Au, ^{181}Au, ^{183}Au, and ^{185}Au.

band is developed to be yrast at high spin and the $h_{9/2}$ and $f_{7/2}$ bands are gradually leaving from the yrast line with decreasing neutron number. As shown in Fig. 4, the transition energies from the $13/2^+$ bandhead of the $i_{13/2}$ band to the $11/2^-$ member of the $h_{9/2}$ band are 558.7, 428.3, and 286.7 keV in ^{185}Au, ^{183}Au, and ^{181}Au, respectively, which stepwise decreases by 130–140 keV with decreasing neutron number. The corresponding transition energy is 145.0 keV in ^{179}Au. Therefore we might expect that the $h_{9/2}$ and $f_{7/2}$ bands in ^{179}Au are located well above the yrast line. Heavy-ion induced reactions mainly populate yrast and near yrast levels, so the $h_{9/2}$ and $f_{7/2}$ bands in ^{179}Au have not been observed in the present work.

The experimental alignments for the $\frac{1}{2}[660](i_{13/2})$ bands in the odd-*A* Au isotopes have been extracted according to Ref. [4] and they are presented in Fig. 5. In such plots, the common Harris parameters $J_0=29.4\hbar^2\ \mathrm{MeV}^{-1}$ and $J_1=121\hbar^4\ \mathrm{MeV}^{-3}$ were used [4]. The band of ^{179}Au has an alignment of about $5.5\hbar$ at low rotational frequency, in agreement with what is expected for an aligned proton state occupying the $\frac{1}{2}[660]$ orbit. The systematics of alignments at low rotational frequency, as shown in Fig. 5, support the configuration assignment to the newly observed band in ^{179}Au.

Comparing the level spaces of the $\frac{1}{2}[660]$ bands in the odd-*A* Au nuclei, one can see that the level spaces are minimized at ^{177}Au and ^{179}Au. This indicates that the $\frac{1}{2}[660]$ bands in ^{177}Au and ^{179}Au have the largest deformation among the known odd-*A* Au nuclei. In Ref. [11], a variable moment of inertia fit was carried out for the $\frac{1}{2}[660]$ bands in the odd-*A* Au nuclei, and empirical values of the deformation were subsequently deduced. The extracted deformations were maximized at neutron numbers of 98 and 100, corresponding to ^{177}Au and ^{179}Au. This result is contradictory to the total Routhian surface prediction, which placed the maximum in deformation near midshell [11]. As stated by Kondev *et al.* [11], such a difference may be due in part to the existence of a deformed subshell gap at $N=98$ as suggested in the Nilsson diagram. This subshell gap might enhance the occupation probabilities of the low-Ω $i_{13/2}$ neutron orbitals and the low-Ω $h_{9/2}$ proton orbitals at $N\sim98$, which is responsible for the magnitude of the deformation of the intruder bands.

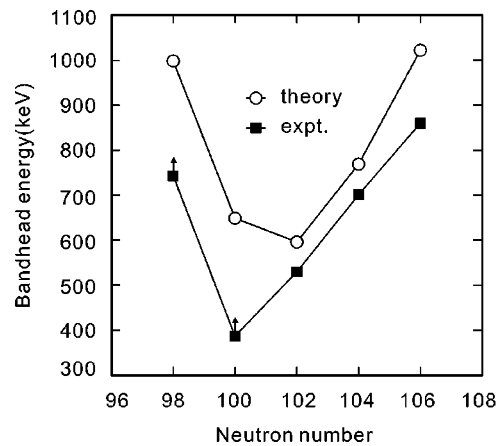

FIG. 6. Experimental and calculated bandhead energies for the $\pi i_{13/2}$ rotational bands in odd-*A* Au nuclei from ^{177}Au to ^{185}Au.

The ground state of ^{179,181,183,185}Au is proposed to be $I^\pi=5/2^-$ and is understood as member of the intruder $\pi h_{9/2}$ band, among which the assignments to ^{179,181}Au have been inferred from the systematics of level structure[4,10,11]. The level spaces between the $9/2^-$ and $5/2^-$ levels of the $\pi h_{9/2}$ bands in ^{183}Au and ^{185}Au are 12.3 and 8.9 keV, respectively [4,10]. Based on the similarity of the partial level schemes shown in Fig. 4, it is reasonable to assume that the lowest level observed in ^{179}Au might be the $9/2^-$ member of the $\pi h_{9/2}$ band and the transition energy between the $9/2^-$ level and the $5/2^-$ ground state is also very small. Thus, the bandhead energy of the $\frac{1}{2}[660](i_{13/2})$ band in ^{179}Au is expected to be around 387 keV. Illustrated in Fig. 6 are the experimental and calculated bandhead energies for the $\frac{1}{2}[660](i_{13/2})$ band from ^{177}Au to ^{185}Au [4]. The calculated bandhead energies are the results from the macroscopic-microscopic shell correction model [4]. In the plot, the experimental bandhead energies in ^{179}Au and ^{177}Au are their lower limits. The calculation predicts that the bandhead energy is lowest at $N=102$, while the experimental minimum is located at $N=100$. Theoretical models should be improved to resolve this difference as well as the discrepancy between the experimental and calculated deformations.

The authors wish to thank the staffs in the JAERI tandem accelerator for providing ^{35}Cl beam. This work was supported by the National Natural Science Foundation of China (Grant No. 10005012) and the Major State Basic Research Development Program of China (Contract No. G2000077402). Y.H.Z. acknowledges support from NNSF (Grant No. 10025525).

[1] K. Heyde, P. van Isacker, M. Waroquier, J. L. Wood, and R. A. Meyer, Phys. Rep. **102**, 293 (1983).
[2] J. L. Wood, K. Heyde, W. Nazarewicz, M. Huyse, and P. van Duppen, Phys. Rep. **251**, 101 (1992).
[3] G. J. Lane *et al.*, Nucl. Phys. **A586**, 316 (1995).
[4] W. F. Mueller *et al.*, Phys. Rev. C **59**, 2009 (1999).
[5] Y. Gono *et al.*, Nucl. Phys. **A327**, 269 (1979).
[6] E. F. Zganjar *et al.*, Phys. Lett. **58B**, 159 (1975).
[7] Y. Gono *et al.*, Phys. Lett. **70B**, 159 (1977).
[8] Ts. Venkova *et al.*, Z. Phys. A **344**, 232 (1992).
[9] N. Perrin *et al.*, Z. Phys. A **347**, 81 (1993).
[10] A. J. Larabee *et al.*, Phys. Lett. **169B**, 21 (1986).
[11] F. G. Kondev *et al.*, Phys. Lett. B **512**, 268 (2001).
[12] J. K. Johansson *et al.*, Phys. Rev. C **40**, 132 (1989).
[13] U. J. Schrewe, P. Tidemand-Petersson, G. M. Gowdy, R. Kirchner, O. Klepper, A. Plochocki, W. Reisdorf, E. Roeckl, J. L. Wood, J. Zylicz, R. Fass, and D. Schardt, Phys. Lett. **91B**, 46 (1980).
[14] K. S. Toth, D. M. Moltz, F. Blonnigen, and F. T. Avignone, Phys. Rev. C **35**, 2330 (1987).
[15] R. B. Firestone, Nucl. Data Sheets **65**, 589 (1992).